Catalysis Letters Vol. 100, Nos. 1–2, March 2005 (© 2005)
DOI: 10.1007/s10562-004-3079-8

n-Octane aromatization on Pt-containing non-acidic large pore zeolite catalysts

Siriporn Jongpatiwuta[a,*], Supak Trakarnroek[a], Thirasak Rirksomboon[a], Somchai Osuwan[a], and Daniel E. Resasco[b]

[a]*The Petroleum and Petrochemical College, Chulalongkorn University, Bangkok, Thailand*
[b]*School of Chemical, Biological, and Materials Science, The University of Oklahoma, Norman, OK, 73019*

Received 27 August 2004; accepted 9 November 2004

Platinum catalysts supported on the potassium-form of different large-pore zeolites (i.e. K-LTL, K-BEA, K-MAZ, and K-FAU) have been tested for *n*-octane aromatization at 500 °C. All catalysts were prepared by the vapor phase impregnation (VPI) method. It was found that the Pt/K-LTL catalyst exhibit a better aromatization performance than the other zeolite catalysts. However, due to secondary hydrogenolysis, the C8 aromatics produced inside the zeolite are converted to benzene and toluene. By contrast, a non-microporous Pt/SiO_2 catalyst did not present the secondary hydrogenolysis. Therefore, despite a lower initial aromatization activity, Pt/SiO_2 results in higher selectivity to C8 aromatics than any of the other zeolite catalysts. All fresh catalysts were characterized by hydrogen chemisorption and FT-IR of adsorbed CO. In addition, the residual acidity of the supports was analyzed by temperature programmed desorption (TPD) of ammonia. In agreement with previous studies, it was found that after reduction at either 350 or 500 °C, the Pt/K-LTL showed much higher Pt dispersion than other catalysts. It is known that the structure of L zeolite can stabilize the small Pt clusters inside the zeolite channel. By contrast, FT-IR indicated that a large fraction of platinum clusters were located outside the zeolite channels in the case of Pt/K-BEA and Pt/K-MAZ catalysts.

KEY WORDS: *n*-octane aromatization; Pt/K-LTL; Pt/K-BEA; Pt/K-MAZ; Pt/K-FAU; Pt/SiO_2; vapor phase impregnation; DRIFTS; catalyst deactivation; TPO; TPD of ammonia; hydrogen chemisorption.

1. Introduction

It is well known that platinum supported on the K form of L zeolite (Pt/K-LTL) is an effective catalyst for *n*-hexane aromatization [1–6]. Many studies have been conducted to understand the uniqueness of this catalyst and its ability to aromatize *n*-hexane [7–14] as well as to improve its tolerance to sulfur, which is a weakness of this unique material [15–22]. A well-recognized fact is that the KL zeolite structure is able to stabilize extremely small Pt clusters (<1 nm) in a completely non-acidic environment, two conditions that are needed in the selective aromatization pathway [23]. In addition to Pt/K-LTL catalysts, several other Pt/zeolites have been investigated as catalysts for *n*-hexane aromatization and many of them showed high activity. However, for a given total conversion, particularly at low conversions, Pt/K-LTL is always the most effective [23,24,25]. Most of the extensive work done on these catalysts has focused on *n*-hexane as a feed. Much less attention has been paid to the aromatization of larger alkanes such as C8, which may also result in valuable aromatic products, such as ethylbenzene and xylenes. Recently, we have investigated the aromatization of *n*-octane over a well-prepared Pt/K-LTL. It is important to qualify this term because in many studies comparisons have been made with Pt/K-LTL catalysts in which a large fraction of the Pt particles were located outside the zeolite channels, as we have previously discussed [26]. By using a variety of characterization techniques, we have demonstrated in several publications that the vapor phase impregnation (VPI) method that we employ results in the majority of the Pt clusters inside the zeolite structure [17,19–21]. Interestingly, although the well-prepared Pt/K-LTL catalysts exhibited a very high selectivity in the aromatization of n-hexane, it did not result in high selectivity to C8-aromatics [26]. In fact, we observed a high concentration of benzene and toluene in the product, which resulted from the secondary hydrogenolysis reaction. A rapid deactivation due to coke deposition was also found; in contrast with a much lower rate of deactivation observed when *n*-hexane was the feed. We explained these dramatic differences in selectivity and stability in terms of diffusional limitations, which become more evident with C8 than with C6 hydrocarbons. Therefore, in this contribution, we have studied the aromatization of *n*-octane over Pt catalysts supported on zeolites of larger pore size. We have investigated K-BEA, K-MAZ, and K-FAU and compared their behavior with that of the KL zeolite. Fresh and spent catalysts were characterized by several techniques e.g. BET, FT-IR of adsorbed CO, hydrogen chemisorption, temperature programed desorption (TPD) of ammonia, and temperature programed oxidation (TPO).

*To whom correspondence should be addressed.

1011-372X/05/0300–0007/0

2. Experimental

2.1. Catalyst preparation

The K-LTL-zeolite (KL; Lot#1041, BET area = 292 m^2/g, SiO_2/Al_2O_3 ratio = 6) was produced by Tosoh Co. NaH-BEA (NaHβ; CP810E, Lot#1822-78) and H-MAZ (HΩ; ZD96026, Lot#2163-53-1) zeolites were produced by Zeolyst International. The Na-FAU (NaY; Type Y-54, Lot#955089001010) zeolite was produced by UOP. A precipitated silica Hi-Sil® 233 (CAS# 7631-86-9, BET area = 140 m^2/g) was provided by PPG Siam Silica Co., Ltd. The zeolites NaH-BEA, H-MAZ, and Na-FAU were exchanged three times with 1 M KNO_3 solution in order to maximize the elimination of protons. The ion exchange process was carried out at 80 °C for 2 h under stirring, using 70 ml per gram zeolite. Prior to addition of the platinum metal, the exchanged zeolites were dried in an oven at 110 °C overnight and then calcined in air flow (100 ml/min. g_{zeol}) at 400 °C for 5 h. Elemental analyses were conducted in a Varian SpectrAA-300 atomic absorption spectrometer. BET surface areas were obtained in a Quantachrome Autosorb-1. The elemental analysis data (Si/Al ratio, K, and Na) together with the BET areas of the bare supports, before Pt impregnation, are summarized in table 1. It can be noted that, except for the K-MAZ, the K-exchanged zeolites exhibited a K/Al ratio close to 1.0, suggesting that the amount of residual acidity should be low. All the Pt/zeolite catalysts were prepared with 1 wt% Pt by VPI, a method that results in high Pt dispersions when the support is an alkaline zeolite [27]. On the other hand, the Pt/SiO_2 catalyst used for comparison was prepared by incipient wetness impregnation (IWI) method. The VPI method is not as effective as IWI for obtaining high dispersions on silica.

In the IWI method, tetraamineplatinum (II) nitrate (Merck) was weighed and dissolved in deionized water (0.69 cm^3/g support) and then impregnated over the dry silica support by slowly dropping the solution under a dry-nitrogen atmosphere. Next, the mixture was dried in an oven at 110 °C overnight. The cool mixture was loaded into a glass tube and calcined at 350 °C in a flow of dry air of 100 $cm^3/min \cdot g$ for 2 h and left to cool to room temperature. The resultant catalyst was stored in a desiccator. All the zeolite catalysts were prepared by the same VPI method that we have used in previous studies [17–19,26]. In this method, weighted amounts of platinum (II) acetylacetonate (Alfa Aesar) and dry support are physically mixed under nitrogen atmosphere. The mixture is then loaded into the reactor tube under a He flow of about 2 cm^3/min. The mixture is slowly ramped to 40 °C and held for 3 h, and ramped again to 60 °C and held again for 1 h. After that pretreatment the temperature is further ramped to 100 °C, at which temperature the mixture is held for 1 h to sublime the $Pt(AcAc)_2$. After sublimation, the mixture is heated to 130 °C and held for 15 min to ensure that the entire precursor is sublimed. After sublimation the sample is heated to 350 °C in flow of air for 2 h to decompose the Pt precursor.

2.2. Catalytic activity measurements

The catalytic activity studies were conducted at atmospheric pressure in a 0.5-inch glass tube with an internal K-type thermocouple for temperature measurement. The reactor was a single-pass, continuous-flow type, with a catalyst bed of 0.20 g. Prior to the reaction, the temperature was slowly ramped in flowing H_2 at 100 $cm^3/min \cdot g$ for 2 h up to 500 °C and *in situ* reduced at that temperature for 1 h. *n*-Octane was added by injection from a syringe pump. In all experiments, the hydrogen to *n*-octane molar ratios was kept at 6:1. The products were analyzed in a Shimadzu GC-17A equipped with a capillary HP-PLOT/Al_2O_3 "S" deactivated column, using a temperature program to obtain optimal product separation.

2.3. Catalyst characterization

The hydrogen uptakes of all catalysts was measured in a static volumetric adsorption Pyrex system, equipped with a high capacity, high vacuum pump that provided vacuum on the order of 10^{-9} torr. Prior to each experiment, 0.4 g of dried fresh catalyst was reduced *in situ* at 350 and 500 °C for 1 h under flowing H_2, cooled down to 300 °C, evacuated to at least 10^{-7} torr at 300 °C for 20 min, then cooled down to room temperature under vacuum. Adsorption isotherms were obtained with

Table 1
Analysis data of Pt catalysts with various supports

Catalyst	BET area of support (m^2/g)	Si/Al mole ratio	K/Al mole ratio	H/Pt (reduced at 350 °C)	H/Pt (reduced at 500 °C)	Amount of NH_3 adsorbed (μmole/g)
Pt/SiO_2	–	–	–	0.38	0.10	43
Pt/K-LTL	300	2.8	0.9	1.20	0.75	54
Pt/K-BEA	660	8.3	1.2	0.24	0.08	185
Pt/K-MAZ	–	2.4	0.6	0.38	0.12	239
Pt/K-FAU	1200	2.1	1.0	0.26	0.22	474
K-FAU	1200	2.1	1.0	–	–	252

several adsorption points ranging from 0 to 100 torr. The H/Pt values were directly obtained by extrapolating to zero pressure.

Fresh and spent catalysts were characterized by DRIFTS using adsorbed CO as a probe in a Nicolet Avatar 360 spectrometer equipped with a DTGS detector. The experiments were performed in a diffuse reflectance cell from Spectra-Tech, type 0030-103 with ZnSe windows. For each IR spectrum, 128 scans were taken at a resolution of 8 cm^{-1}. Prior to taking each spectrum, a background was collected on the sample reduced *in situ* under a flow of H_2 at 500 °C for 1 h and purged in He for 30 min at room temperature. Then, a flow of 3% CO in He for 30 min was sent over the sample, followed by a purge in He flow for 30 min. After this treatment, the spectrum of adsorbed CO was collected.

To determine the concentration of residual acid sites that remain on the zeolite after the K-exchange, TPD of adsorbed ammonia was carried out in a 1/4'' quartz fixed bed reactor. Fifty milligram of zeolite sample was placed in the reactor and heated (3 °C/min) under He flow (30 ml/min) up to 500 °C for 1 h in order to remove water and clean up the catalyst surface. The reactor was then cooled down to 100 °C, which was the adsorption temperature. Then, the sample surface was saturated by flowing of 10% NH_3/He (30 ml/min) for 30 min. After purging by He (30 ml/min) for 2 h to eliminate non-adsorbed and weakly held NH_3 molecules, the sample was heated linearly at 10 °C/min to 800 °C under the same He flow. The evolved ammonia was analyzed on-line with a TCD detector.

TPO was employed to analyze the amount and characteristics of the coke deposits left on spent catalysts after the aromatization reaction. The highly sensitive TPO system was set up as previous reported [28]. TPO of the spent catalysts were obtained in a continuous flow of 2% O_2/He while the temperature was linearly increased at 12 °C/min. The 0.03 g sample was dried at 110 °C overnight and weighed before placing it in a 1/4'' quartz fixed-bed reactor. It was then exposed to 2% O_2 in He for 30 min at room temperature before starting the temperature ramp. The CO_2 produced by the oxidation of coke species was further converted to methane on a 15% Ni/Al_2O_3 catalyst in the presence of hydrogen at 400 °C. The methane thus obtained was analyzed online by a FID detector. The amount of oxidized coke was calibrated by using 100 μl pulses of pure CO_2.

3. Results and discussion

3.1. Characterization of the Fresh Catalysts

The hydrogen uptake (H/Pt) obtained on the Pt/silica and the Pt/zeolite catalysts after reduction at 350 and 500 °C are shown in table 1. For all the catalysts, the H/Pt value decreased when the reduction temperature increased. The Pt/K-LTL exhibited the highest H/Pt while Pt/K-BEA showed the lowest. In agreement with previous studies [23,29,30], a unique property of K-LTL is its ability of stabilizing small Pt clusters, which results in high hydrogen uptakes.

The DRIFTS of CO adsorbed on Pt/SiO_2, Pt/K-LTL, Pt/K-BEA, Pt/K-MAZ, and Pt/K-FAU are illustrated in figure 1. As reported previously [20,26], the adsorption of CO on small Pt clusters inside the L-zeolite channels leads to the formation of Pt carbonyls, which result from a disruption of the Pt clusters by interaction with CO. These Pt carbonyls are stabilized inside L-zeolite channels and exhibit characteristic IR adsorption bands below 2000 cm^{-1}. On the other hand, when the catalyst contains Pt clusters outside the zeolite channels, a clear shoulder is evident at 2070 cm^{-1}. The band between 2050 and 2000 cm^{-1} were related to CO adsorbed on particles near the pore mouth. It is interesting to note, that only the Pt/K-LTL catalyst exhibited the bands below 2000 cm^{-1}, which represents highly disperse Pt inside the zeolite channel. The spectra of adsorbed CO on Pt/K-MAZ and Pt/K-BEA catalysts are centered at 2075 cm^{-1}, which is similar position to that of non-microporous Pt/SiO_2 catalysts. The position

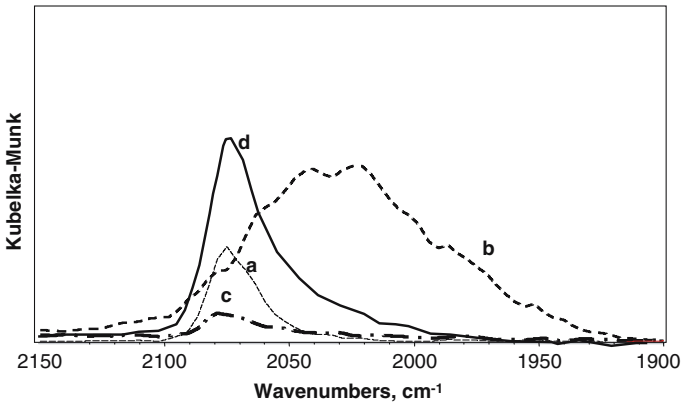

Figure 1. DRIFTS spectra of CO adsorbed on fresh catalysts reduced *in situ* at 500 °C. The reduced catalysts were exposed to a flow of 3% CO in He for 30 min at room temperature and purged in He for 30 min. (a) Pt/SiO_2, (b) Pt/K-LTL, (c) Pt/K-BEA, and (d) Pt/K-MAZ.

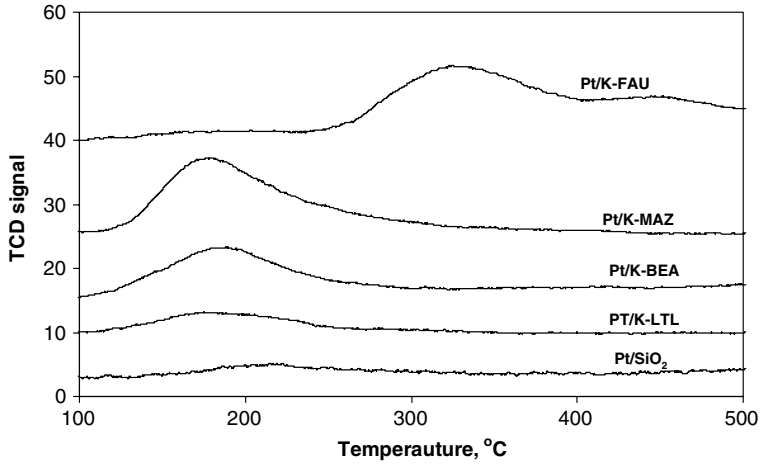

Figure 2. TPD profiles of ammonia adsorbed at 100 °C on the Pt catalysts with different supports.

of this band and the low hydrogen uptakes obtained on these catalysts indicate that these zeolites are not able to stabilize a large fraction of Pt clusters inside the pore structure, but rather have the metal particles as large aggregates on the outer surface of the crystals.

The TPD profiles and total amount of adsorbed ammonia at 100 °C on the different catalysts are shown in figure 2 and table 1, respectively. The Pt/SiO_2 and Pt/K-LTL catalysts exhibited an extremely low residual acidity while Pt/K-BEA and Pt/K-MAZ exhibited some extent of weakly adsorbed NH_3. In these catalysts, the adsorbed NH_3 desorbed below 250 °C, which shows that the residual acidity on these supports, if any, is weak. The only sample which exhibited desorption above this temperature was the Pt/K-FAU, indicating the presence of strong acid sites. As mentioned above, the K-MAZ zeolite exhibited a rather low K/Al ratio, which indicates that some residual protons were left behind after the exchange. By contrasts, the Pt/K-FAU showed a much higher adsorption of strongly adsorbed NH_3, while the K analysis indicated a high degree of ion exchange. It is possible that at least a fraction of these sites may have been generated during the metal impregnation and activation steps. It has been proposed that acid sites are generated during the reduction in hydrogen of the Pt precursors [22]. However, the enhancement in acidity density shown in table 1 for the Pt/K-FAU compared to the K-FAU support occurred after calcination at 350 °C, before any reduction.

3.2. Catalyst activity

The Pt/SiO_2, Pt/K-LTL, Pt/K-BEA, Pt/K-MAZ, and Pt/K-FAU catalysts were tested for *n*-octane aromatization at 500 °C as a function of time on stream. The *n*-octane conversion and total aromatics selectivity obtained on each catalyst are shown in figure 3a and b, respectively. It was observed that the Pt/K-LTL exhibited the highest activity and total aromatics selectivity among the different zeolite-supported catalysts. However, the activity for this catalyst rapidly dropped at about 6 h on stream. In our previous study [26], we have noted that this drop is due to pore plugging and does

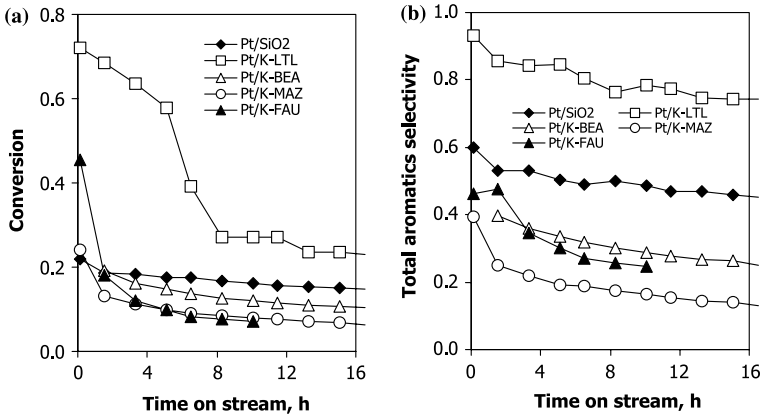

Figure 3. (a) *n*-Octane conversion and (b) Total aromatics selectivity (mole basis) versus time on stream over Pt/SiO_2 and Pt/zeolite catalysts. Reaction conditions: 500 °C, H_2/ *n*-C8 molar ratio 6:1,WHSV 5 h^{-1}.

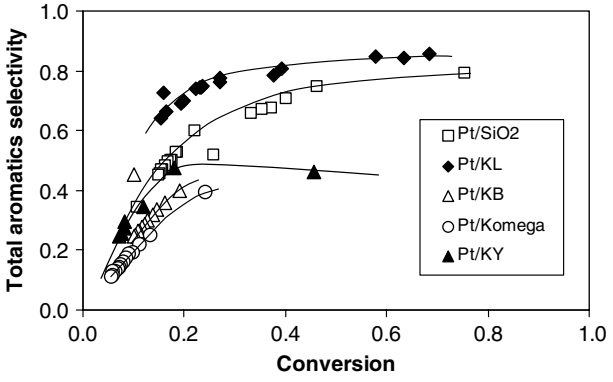

Figure 4. Total aromatics selectivity (mole basis) versus total *n*-C8 conversion over Pt/SiO_2, Pt/K-LTL, Pt/K-BEA, Pt/K-MAZ, and Pt/K-FAU catalysts. Reaction conditions same as figure 3.

not occur when the feed is *n*-hexane. An even more pronounced deactivation was observed on the Pt/K-FAU catalyst with drastic losses in both activity and selectivity to aromatics. The rest of the zeolite catalysts, Pt/K-BEA, and Pt/K-MAZ exhibited even lower activity, stability, and total aromatics selectivity than the silica-supported catalyst. In fact, it is seen that among these catalysts, the silica-supported Pt catalyst appears as a rather effective C8 aromatization catalyst.

Figure 4 shows the plot of selectivity to total aromatics versus conversion obtained on the different catalysts. It was observed that while for all the catalysts the selectivity increased with conversion, the Pt/K-LTL exhibited the highest aromatization selectivity at a given conversion. However, as shown in table 2, the distribution of products from this catalyst after 10 h on stream showed that the dominant aromatics were benzene and toluene. We have previously demonstrated that benzene and toluene obtained on this catalyst are secondary products resulting from the hydrogenolysis of the previously formed C8-aromatics [26]. The proposed reaction pathway is shown in Scheme 1. Even though the

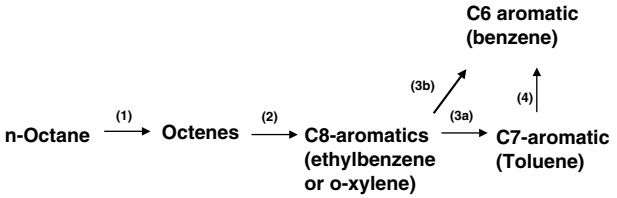

Scheme 1. Proposed reaction pathway for *n*-octane aromatization followed by hydrogenolysis.

non-microporous Pt/SiO_2 showed less total aromatics selectivity than Pt/K-LTL (figure 4), it did not favor the secondary hydrogenolysis of the C8-aromatics, resulting in the highest selectivity to C8-aromatics within the series of catalysts investigated. Furthermore, the selectivity to C8 aromatics on this catalyst is highest at high conversions. The detailed product distribution analysis showed that ethylbenzene (EB) and *o*-xylene (OX) were the dominant products among the C8 aromatics for all the catalysts. Among the zeolites, Pt/K-BEA and Pt/K-MAZ resulted in higher C8-aromatics than Pt/K-LTL but less than Pt/SiO_2. By contrast, the Pt/K-FAU catalyst exhibited high concentration of benzene and toluene and low C8-aromatics, indicating a similar secondary hydrogenolysis reaction as that previously observed on Pt/K-LTL [26]. The Pt/K-MAZ catalyst, which exhibited the lowest K/Al ratio, and a relatively high density of residual (weak) acid sites, resulted in rapid deactivation and high concentration of cracking and C8 isomerization products (*m*- and *p*-xylenes).

Figure 5 shows the evolution of the selectivity to the various aromatic products as a function of conversion. The simplest case to analyze is the non-microporous Pt/SiO_2. On this catalyst, there is no secondary hydrogenolysis and it is clearly seen that the selectivity to C8-aromatics increases with conversion, at the expense of the octenes. Octenes are dehydrogenation intermediates that are quickly produced at low conversions, but are then consumed in the subsequent aromatization.

Table 2
Product distribution of *n*-octane aromatization on Pt/SiO_2 and Pt/zeolite catalysts, after 10 h on stream

	Pt/SiO_2	Pt/K-LTL	Pt/K-BEA	Pt/K-MAZ	Pt/K-FAU
Conversion	16.2	37.7	12.1	8.0	7.2
Product selctivity, %wt					
C1–C5	7.4	29.4	10.3	19.8	17.2
C6–C7	0.9	1.2	5.1	6.7	4.9
Octenes	42.6	3.9	55.1	56.9	40.1
Benzene	0.0	27.7	0.1	1.7	3.8
Toluene	0.0	26.8	1.8	2.1	19.7
EB	22.3	6.5	14.9	6.8	10.0
m-, *p*-Xylene	1.5	1.4	1.7	2.0	0.0
o-Xylene	24.7	3.0	11.4	4.8	4.3
Total Aromatics	48.5	65.3	28.6	15.4	37.8
Total C8-Aromatics	48.5	10.9	26.7	11.6	14.3

Reaction conditions; 500 °C, H_2: *n*-C8 ratio 6:1, WHSV 5 h^{-1}.

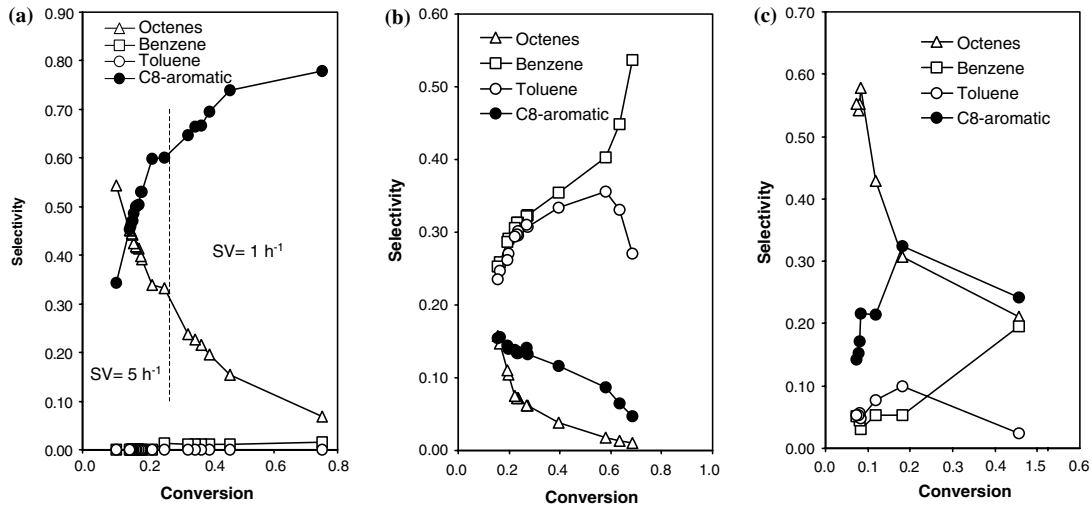

Figure 5. Product selectivities versus total *n*-C8 conversion during *n*-octane aromatization over (a) Pt/SiO2, (b) Pt/K-LTL, and (c) Pt/K-FAU catalysts. Reaction conditions same as figure 3, except for the high conversion part of (a), which was conducted at a space velocity of 1 h^{-1}.

Therefore, the differences in octene selectivity are due to differences in the ability of each catalyst in converting olefins to aromatics. On the Pt/K-LTL, the aromatization of the olefins is so rapid that there is little build up of octenes. At the same time, on this catalyst, the selectivity to C8-aromatics decreased as conversion increased, while toluene and benzene increased, due to the sequential hydrogenolysis. Furthermore, at a conversion higher than about 60, the selectivity to toluene also started decreasing, while benzene concentration more quickly increased and ended up being the dominant product at high conversions. Likewise, the Pt/K-FAU exhibited the secondary hydrogenolysis reaction, also producing more benzene at high conversion. Moreover, this catalyst exhibited another detrimental feature that is a high level of cracking, which also increased with conversion. As a result, it can be expected that the total aromatic concentration on the Pt/K-FAU catalyst reaches a maximum at low conversions and then decreases.

In our previous contribution [26], we put forward a method of using the EB/OX ratio as an indication of mass transfer limitations inside the channels of the zeolite. It was found that on Pt/SiO_2 and other non-zeolitic supports the EB/OX ratio was unity and no benzene or toluene was found in the product. This result was explained taking into account that, when secondary hydrogenolysis is not present, similar quantities of EB and OX are produced over Pt. However, when the primary products react further, the molecule that remains longer inside the pore of the zeolite is consumed to a greater extent. In this case, OX with a larger kinetic diameter has a much greater difficulty in leaving the pore after it has been produced than EB. As a result, a high EB/OX ratio indicates that both of them have been produced inside the channels of the zeolite, but OX has been preferentially consumed.

In previous studies [17–21], we have observed very low deactivation and very small changes in selectivity over Pt/KL catalyst when C6 was used as a feed. Only when we switched to a C8 feed, both, deactivation and selectivity changes became much more pronounced. The only difference between the two cases is the extent of coking. Therefore, we ascribed coking as the main responsible for the selectivity changes as a function of time. As shown in figure 6, the EB/OX ratio obtained from C8 feed over the Pt/KL catalyst not only is greater than the one on Pt/SiO_2 from the start, but it also increases as a function of time on stream. This increase may be due to an enhancement of the diffusional limitations inside the zeolite channel as coke gradually restricts the molecular transport, making it increasingly difficult for OX to leave. Very similar increases in the EB/OX ratio as a function of time on stream were observed for Pt/K-MAZ and Pt/K-FAU. The increases in this ratio was slow for Pt/K-LTL and Pt/MAZ, which are one dimensional pore structure zeolites, while it was more drastic for Pt/K-FAU (i.e., from 1.5 to 2.2 in only 9 h on stream). This drastic variation may be associated with the much greater amount of coke produced on this catalyst. By contrast, over Pt/SiO_2 the EB/OX ratio was constant as a function of time on stream and about 1.0. Similarly, on Pt/K-BEA, the ratio was constant with time on stream but at a value of 1.5. The unchanged EB/OX on Pt/K-BEA indicates that either the diffusion conditions do not change as a function of time or EB and OX are formed outside the zeolite structure. The former is consistent with the very small amounts of coke formed during reaction while the latter would result in an EB/OX ratio of about 1.0, as is seen on the non-microporous catalysts. The observed EB/OX ratio of 1.5, but this higher value may be a result of a secondary xylene isomerization that would decrease OX by con-

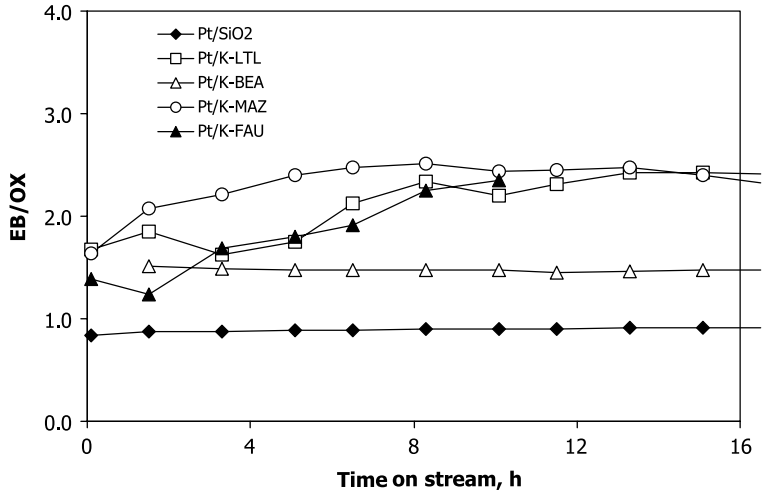

Figure 6. Ethylbenzene: *o*-Xylenes ratio as a function of time on stream during the aromatization of *n*-octane over Pt/SiO_2, Pt/K-LTL, Pt/K-BEA, Pt/K-MAZ, and Pt/K-FAU catalysts. Reaction conditions same as figure 3.

verting to *m*- and *p*-xylenes. If all the xylenes are considered as coming from OX, then the original EB/OX ratio would be 1.25, which is close to one.

Our results show that Pt/K-LTL is unique for *n*-octane aromatization among non-acidic large pore zeolite catalysts, in a similar way as it is unique in the *n*-hexane aromatization. However, there are some important differences between the two reactions. In the first place, when *n*-octane is the feed, two undesired secondary reactions affect the performance of Pt/K-LTL, coke and hydrogenolysis. Although these two reactions are practically negligible with *n*-hexane, they become detrimental to both selectivity and deactivation with *n*-octane feeds. There are also differences with other zeolites. For example, in a previous study [7], it was found that the Pt/K-MAZ, which is structurally similar to Pt/K-LTL (unidimensional pore system, aperture of 7.1 Å for LTL and 7.4 Å for MAZ), exhibited similar activity and benzene selectivity in the aromatization of *n*-hexane. However, in the present work the Pt/K-MAZ exhibits much poorer ability than Pt/K-LTL for the aromatization of *n*-octane. At 10 h on stream, Pt/K-MAZ resulted in 15% aromatics with 8% conversion while Pt/K-LTL exhibited 66% aromatic with 38% conversion (table 2). H/Pt ratio after reduction at 500 °C indicates that Pt/K-MAZ is one-sixth active platinum surface compared to Pt/K-LTL (table 1). Moreover, the results from DRIFTS of adsorbed CO indicate that Pt clusters on K-MAZ are most probably located outside the zeolite. In addition, Pt/K-BEA in which the structure is two-dimensional pore system with aperture of 6.7 Å also exhibited Pt cluster outside zeolite channel and resulted in lower activity and total aromatic selectivity than Pt/K-LTL. From the analysis of the EB/OX ratio, it can be inferred that aromatization reaction on this Pt/K-BEA catalyst mostly occurred on the outer surface of the zeolite. Regarding the Pt/K-FAU catalyst, the TPO results indicate that the drastic drops in activity and selectivity to aromatics were due to coke formation, related to the 3-dimensional pore system and the high residual acidity of the FAU zeolite. The participation of residual strong acid sites was made evident by the considerable amount of C1-C5 cracking products (table 2). Similar to Pt/K-LTL, the *n*-octane aromatization on Pt/K-FAU was followed by secondary hydrogenolysis of the C8 aromatics producing benzene and toluene.

3.3. Characterization of spent catalysts

All spent catalysts were analyzed by TPO after reaction to study the nature and amount of the coke deposited during the reaction. The TPO profiles of the coke deposits on each different catalyst are reported in figure 7. The weight percent of the coke deposits on Pt/SiO_2, Pt/K-LTL, Pt/K-BEA, Pt/K-MAZ, and Pt/K-FAU were 0.87, 1.51, 1.92, 0.92, and 8.30, respectively. Iglesia *et al.* [31,32] have shown that in the case of *n*-hexane aromatization, the well-dispersed Pt clusters located inside the channels of the L zeolite are effectively protected from coke formation by the inhibition of the bimolecular collisions that lead to coke. In the case of *n*-octane, we have shown [26] that the coke precursors are most probably the C8 aromatic products, which slowly diffuse within the zeolite.

As described previously, Pt clusters can accelerate the oxidation of coke and this catalyzed oxidation affects the shape and peak position in the TPO profiles. In this case, the coke oxidized at low temperatures can be ascribed to accessible carbon located next to Pt clusters. In contrast, the high-temperature bands (300–650 °C) are possibly due to the plugging of zeolite pores [26], which would retard the oxidation of the coke deposits. From the figure, BEA and MAZ spent catalysts only exhibited low-temperature peaks similar to those of coke

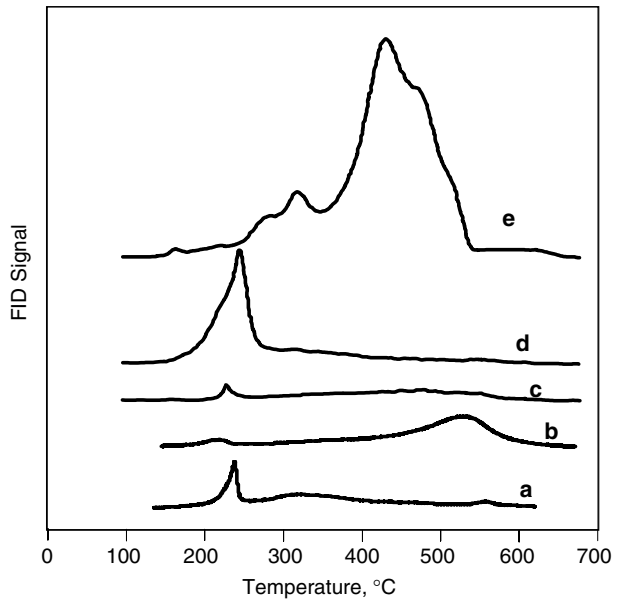

Figure 7. TPO profiles of coke deposits on (a) Pt/SiO_2, (b) Pt/K-LTL, (c) Pt/K-BEA, (d) Pt/K-MAZ, and (e) Pt/K-FAU, after reaction at 500 °C for 10 h on stream.

deposited on Pt/SiO_2. It is possible that Pt clusters over K-BEA and K-MAZ are mostly outside the zeolite channel and the reactions occurred on these platinum clusters leading to coke deposits outside the zeolite channel. The TPO of the spent Pt/KL shows that while this catalyst produces a small amount of coke, this coke oxidizes at a rather high temperature, indicating that it might be located well inside the zeolite and it may indeed be coming from C8 aromatic precursors that remained trapped inside the zeolite.

It is worth noting that the spent Pt/K-FAU catalyst exhibited much higher concentration of coke deposits than any of the other zeolite catalysts. It is possible that the FAU structure and the rather high acidity density generated during Pt deposition are more conducive to coking than the other zeolites.

It is clear that coke prevention alone is not sufficient to promote high aromatization selectivity, the location of the platinum clusters and morphology of support is important for enhancing the aromatization performance.

4. Conclusions

Among the Pt-containing large pore zeolites studied in this work, the Pt/K-LTL catalyst exhibits the best performance for the aromatization of *n*-octane. Even though the aperture size of MAZ is larger than LTL, the Pt/K-MAZ exhibited much lower activity and selectivity to aromatics than Pt/K-LTL. Pt dispersion and location are important factors to the aromatization performance. Similar to the case of *n*-hexane aromatization, the uniqueness of Pt/K-LTL may be mostly due to its ability to stabilize Pt clusters inside its channel structure under reduction conditions. However, when using n-C8 alkanes as feed, the selectivity to C8 aromatics is drastically reduced by secondary hydrogenolysis to benzene and toluene that occurs inside the zeolite pores. As a result, a non-microporous non-acidic support such as silica turns out to be the one that imparts the highest selectivity to C8 aromatics. Although its initial aromatization activity is not high and it produces high concentration of olefins at low and intermediate conversions, it can be very selective at high conversions and does not favor secondary hydrogenolysis.

Acknowledgments

This work was supported by The Thailand Research Fund (TRF) under the Royal Golden Jubilee Ph.D. program and basic research project. Part of the experimental work was supported by the Oklahoma Center for the Advancement of Science and Technology (OCAST) and ConocoPhillips.

References

[1] J.R. Bernard, *Proceedings in 5th International Conference on Zeolite*, ed. L.V.C. Rees (Heyden, London, 1980), 686.
[2] T.R. Hughes, W.C. Buss, P.W. Tamm and R.L. Jacobson, Stud. Surf. Sci. Catal. 28 (1986) 725.
[3] T.R. Hughes, D.H. Mohr and C.R. Willson, Stud. Surf. Sci. Catal. 38 (1987) 335.
[4] D.V. Law, P.W. Tamm and C.M. Detz, *AIChE Meeting* (Houston, TX, USA, March 29, 1987).
[6] C. Besoukhanova, C.M. Breysse, J.R. Bernard and D. Barthomeuf, *Catalyst Deactivation* (1980) 201.
[6] T.R. Hughes, W.C. Buss, P.W. Tamm and R.L. Jacobson, *AIChE Meeting* (New Orleans, LA, USA, April 8, 1986).
[7] J.T. Miller, N.G.B. Agrawal, G.S. Lane and F.S. Modica, J. Catal. 163 (1996) 106.
[8] R.E. Jentoft, M. Tsapatsis, M.E. Davis and B.C.J. Gates, J. Catal. 179 (1998) 565.
[9] S.J. Tauster and J.J. Steger, J. Catal. 125 (1990) 387.
[10] J.T. Miller and D.C. Koningsberger, J. Catal. 162 (1996) 209.
[11] P.V. Menacherry and G.L. Haller, J. Catal. 177 (1998) 175.
[12] T. Fukunaga and V. Ponec, J. Catal. 157 (1995) 550.
[13] E.G. Derouane and D.J. Vanderveken, Appl. Catal. 45 (1988) L15.
[14] C. Besoukhanova, J. Guidot, D. Barthomeuf, M. Breysse and J.R. Bernard, J. Chem. Soc. Faraday Trans. 1(77) (1981) 1595.
[15] X. Fang, F. Li, O. Zhou and L. Luo, Appl. Catal. 161 (1997) 227.
[16] X. Fang, F. Li and L. Luo, Appl. Catal. 146 (1997) 297.
[17] G. Jacobs, W.E. Alvarez and D.E. Resasco, Appl. Catal. 206 (2001) 267.
[18] S. Jongpatiwut, P. Sackamduang, T. Rirksomboon, S. Osuwan, W.E. Alvarez and D.E. Resasco, Appl. Catal. 230 (2002) 177.
[19] G. Jacobs, C.L. Padro and D.E. Resasco, J. Catal. 179 (1998) 43.
[20] G. Jacobs, F. Ghadiali, A. Pisanu, C.L. Padro, A. Borgna W.E. Alvarez and D.E. Resasco, J. Catal. 191 (2000) 116.
[21] G. Jacobs, F. Ghadiali, A. Pisanu, A. Borgna, W.E. Alvarez and D.E. Resasco, Appl. Catal. 188 (1999) 79.

[22] D.J. Ostgard, L. Kustov, K.R. Poeppelmeier and W.M.H.J. Sachtler, J. Catal. 133 (1992) 342.
[23] W. Mielczarski, S.B. Hong, R.J. Davis and M.E. Davis, J. Catal. 134 (1992) 359.
[24] A.W. Chester, J. Catal. 86 (1984) 16.
[25] G.S. Lane, F.S. Modica and J.T. Miller, J. Catal. 129 (1991) 145.
[26] S. Jongpatiwut, P. Sackamduang, T. Rirksomboon, S. Osuwan, W.E. Alvarez and D.E. Resasco, J. Catal. 218 (2003) 1.
[27] A.E. Schweizer (Exxon) US Patent 4,992,401 (1991).
[28] S.C. Fung and C.A. Querini, J. Catal. 138 (1992) 240.
[29] S.B. Hong, W. Mielczarski and M.E. Davis, J. Catal. 134 (1992) 349.
[30] M. Ballatreccia, R. Zanonin, C. Dossi, R. Psaro, S. Recchia and G. Vlaic, J. Chem. Soc. Farad. Trans. 91 (1995) 2045.
[31] E. Iglesia and J.E. Baumgartner, *Proc. IX Internat. Zeolite. Conf.*, Montreal (1992).
[32] E. Iglesia and J.E. Baumgartner, *Proc. X Internat Congr. Catal.*, eds. L. Guczi *et al.* (Elsevier Sci. Publ., New York, 1993) 993.